J. Fluid Mech. (1974), *vol.* 64, *part* 2, *pp.* 227–239
Printed in Great Britain

Turbulent vortex rings†

By T. MAXWORTHY

Departments of Aerospace and Mechanical Engineering, University of Southern California, Los Angeles, California 90007

(Received 29 June 1973 and in revised form 17 December 1973)

We consider the motion of the mass of fluid ejected through a sharp-edged orifice by the motion of a piston. The vorticity formed by viscous forces within the separated flow at the sharp edge rolls up to form a concentrated vortex which, after a development period, consists of a core of very fine scale turbulence surrounded by a co-moving bubble of much larger scale turbulence. This bubble entrains outer fluid, mixes with it, and deposits the majority into a wake together with some small fraction of the total vorticity of the ring. Enough fluid is retained to account for the slow growth of the whole fluid mass. A theory which takes account of both the growth process and the loss of vorticity is proposed. By comparison with experimental measurements we have determined that the entrainment coefficient for turbulent vortex rings has a value equal to $0{\cdot}011 \pm 0{\cdot}001$, while their effective drag coefficient is $0{\cdot}09 \pm 0{\cdot}01$. These results seem to be independent of Reynolds number to within experimental accuracy.

1. Introduction

Vortex rings have been the subject of several recent investigations. The interest seems to be based mainly on potential industrial applications although the basic fluid mechanics involved has also come in for its share of attention. It is the latter that we emphasize here, but hope that our results will be of use to those with technological applications in mind. Among the latter are, first, a desire to use rings to transport industrial waste to high altitudes (Turner 1960). A brief comment on this is given at the end of § 2. Second, the increased interest in the trailing vortex pair that exists behind a lifting surface has spawned a general effort in vortex dynamics. There seems to be some hope that an understanding of the more readily produced vortex ring will result in a better feeling for the processes involved in the aircraft wake problem. We share this feeling and hope to make a contribution to this subject at a later date. We also believe that vortex rings, though not necessarily those treated here, will serve as a useful model for the elements of turbulence in complicated high Reynolds number flow problems.

Most of the work on the initial stages of development of the vortex ring formed at a sharp-edged orifice has been performed by Krutsch (1939), Sullivan, Widnall & Ezekiel (1973) and Widnall & Sullivan (1973), although some relevant comments have been made by Maxworthy (1972). In the present work, the motion of

† With an appendix on an extended theory of laminar vortex rings.

primary interest is that which takes place after these initial phases have passed. It has been closely observed by only a few investigators, and even now, is not completely understood. We hope partially to remedy this situation by describing this motion and by proposing a theoretical model which seems to be consistent with experimental observations.

Johnson (1970, 1971) has published some data, but his interpretation is difficult to reconcile with the results we shall present. Further comments follow in § 5.

The results presented here depend heavily on the concepts developed by the present author for laminar vortex rings (Maxworthy 1972) and an appendix on the extension of that theory is presented to round out our discussion.

2. Experimental procedure and some preliminary observations

The apparatus shown in figure 1 was used to study the properties of turbulent vortex rings in the Reynolds number RU/ν† range $0{\cdot}5 \times 10^4$–$1{\cdot}5 \times 10^4$.

Rings were formed by pushing on the piston of the generator, displacing fluid through the hole. Vorticity was created at the sharp edge and this rolled up to form a concentrated vortex. Ring velocity and size could be varied over a wide range by varying the force with which the piston was pushed and by varying the volume of fluid displaced. Two hole diameters (3 and 5 cm) were also used in a series of tests designed to determine the character of the flow and to test the theoretical model derived from these observations.

The sequence of events that occurs during any one experiment is illustrated on figure 1. When the piston of the generator is pushed, a blob of fluid emerges from the hole. It rolls up into the form of an oblate spheroid‡ owing to the self-induction of the vorticity produced at the edge of the hole (figure 2, plate 1). The vorticity distribution which results is highly peaked, but there are small amounts all the way out to the edge of the moving fluid mass (Sullivan *et al.* 1973; Maxworthy 1972). Some finite portion of the central concentrated region then becomes unstable to short wavelength disturbances (there being typically 12 waves around the core in our case) (Widnall & Sullivan 1973; Maxworthy 1972).§ These instabilities grow to finite amplitude and then go through a tumbling or breaking process.

† Where R is the radius of the ring defined in figure 1 and more clearly in figure 6(*a*). U is the ring velocity and ν the kinematic viscosity of the fluid.

‡ This moving fluid mass is variously called a bubble or ring in what follows. The latter name is unfortunate because it does not accurately describe the geometry; however, historical precedent requires that we use this term occasionally, and we hope it causes no confusion.

§ There are currently two possible explanations for the occurrence of these unstable waves. Widnall & Sullivan (1973) suggest a short wavelength instability of the core flow. Their theory is, unfortunately, only valid if the wavelength of the disturbance is larger than the core diameter, which is not true experimentally. The ultimate flow which emerges in the tests should also be unstable according to their theory, but is not! Moore & Saffman (1973, private communication) have attempted a small perturbation analysis with inconclusive results, but a suggestion that the flows considered by Widnall & Sullivan are stable. Recently Prof. Widnall has extended her stability theory to include short wave-

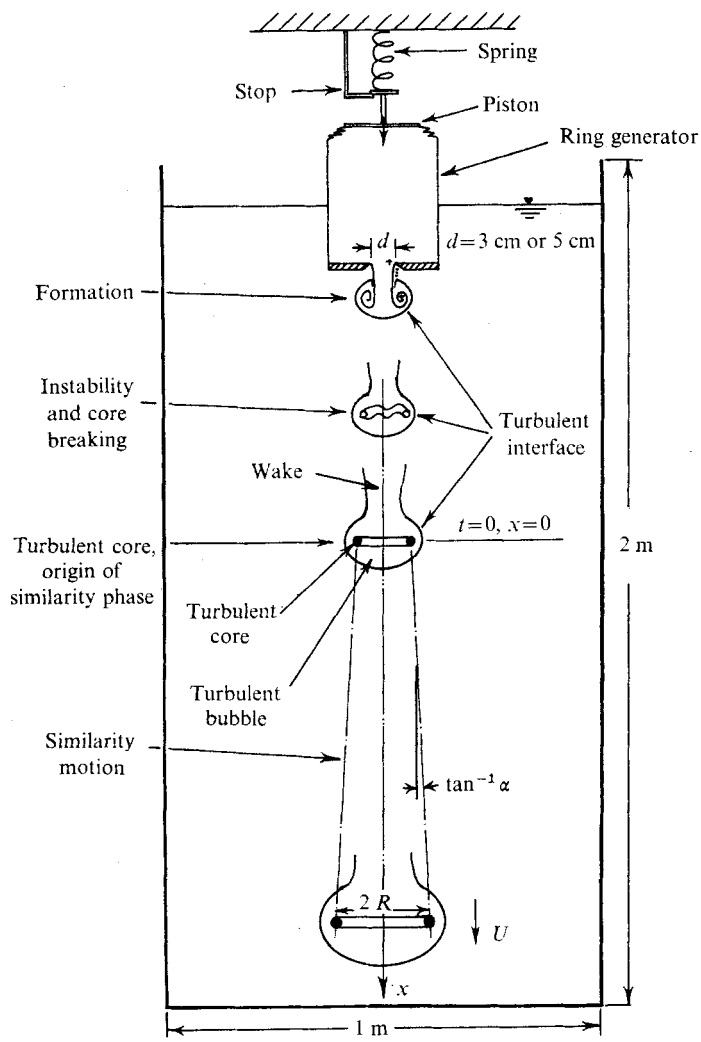

FIGURE 1. Apparatus. Showing sequence of events creating a turbulent vortex ring.

At about this stage in the ring's motion, the curve of distance x travelled by the ring *vs.* time t or alternatively, ring velocity U *vs.* x undergoes a rapid change in slope. For example, if one plots these curves on semi-logarithmic graph paper, both the motion before and the motion after instability are close to straight lines, but each with a different slope (Krutsch 1939; Maxworthy 1972; Widnall 1973, private communication). In Maxworthy (1972), it was erroneously assumed

length disturbances and realistic vorticity distributions, finding better agreement with experimental results. Maxworthy's (1972) suggestion that vorticity of opposite sign to that of the main core is swept into the vortex bubble to produce conditions conducive to Rayleigh–Taylor instability is an attractive but unproven alternative. Hopefully, further work will unravel these difficult problems. For present purposes, all we need know is that such an instability does exist and that it leads to a turbulent core in the final stages of ring motion.

that because of this exponential behaviour both before and after instability the mechanism describing each regime was the same. It is clear from the present work that this is not so, and that even though the general features of entrainment are similar, the details are not.

The fluid participating in the instability ends up as a rapidly rotating core of very fine scale turbulence† for which the ratio R/a‡ remains constant at a value of approximately 10 as the ring propagates (Johnson 1970). As in most rapidly rotating flow, the turbulent fluctuations perpendicular to the axis of rotation are suppressed. This means that the interface between the core and its surroundings is only slightly contorted and it entrains fluid very slowly, as the measurements will show. It is this process which controls the overall growth rate of the ring. At the same time, vorticity is being removed from the ring and being deposited into the surrounding fluid bubble, from which it eventually finds its way into a wake. During this process, the outer region of the spheroid has also become turbulent;† however, the mean vorticity within it is low and the turbulent scales are large, being a substantial fraction of the size of the spheroid. This region, in a sense, processes entrained fluid. Fluid is entrained by the large-scale corrugations of the interface and mixes with interior fluid. Most of it is then rejected to the wake and only a small amount retained, enough to account for the very slow growth of the core and the turbulent spheroid. These processes can be demonstrated in three ways. In the main set of experiments, a compact blob of dye was ejected from the orifice (figure 3, plate 2). The outer region immediately began entraining ambient fluid, mixing with it and depositing the mixture into the wake. The dye concentration in the outer regions became more and more dilute, leaving only the slowly growing core with any dye at all. In the second, less extensive set of experiments, an undyed blob of fluid was ejected from the generator and was allowed to propagate through dyed ambient fluid. The resulting flow is shown in figure 4 (plate 3) and a sketch in figure 7 (*a*). The outer region of the moving bubble was immediately filled with dyed fluid, but the core remained clear. As time progressed, a thin skin around the core became dyed (figure 7*a*), but penetration to the centre of the core never seemed to take place, at least during our experiments. The third experiment was undertaken to try to get some idea of the relative scales of turbulence in the two regions. A weak salt solution was ejected into the tank and the resulting density field observed using a shadowgraph apparatus. Figure 5 (plate 3) shows a photograph taken using such a system. The fluid density is low enough and it is early enough for the ring dynamics to be dominated by the initial impulse. The extent of the outer bubble can be clearly seen, as can the interface between it and the inner ring. The focusing effect of this ring tends to obscure the turbulence structure, but visual observations show it to be small. The *major* motions in the outer bubble are of larger scale; they mix environmental fluid with bubble fluid and deposit the majority into the wake. There are, clearly, small-scale streaks in the region,

† Until more detailed measurements are undertaken, the actual magnitudes of these turbulent quantities can only be conjectured. From our visual impressions of the flow, the major scale in the core was about $\frac{1}{4}a$, while that in the bubble was about $\frac{1}{4}R$.

‡ R is the main radius of the toroidal ring and a its minor radius (see figure 6*a*).

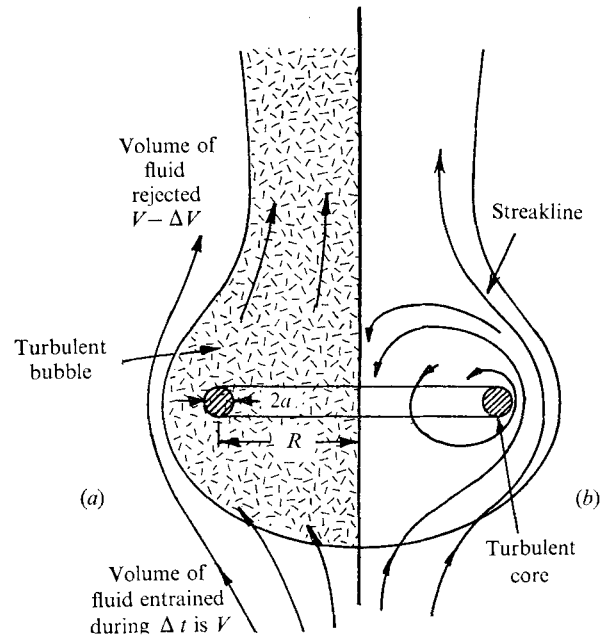

FIGURE 6. (*a*) Showing the outer regions of the moving fluid mass as a processor of ambient fluid. A large amount V is entrained, but most is rejected to a wake. (*b*) Streaklines for the turbulent ring.

but they are being convected around and stretched by the large scales, and only show up because of the small diffusion coefficient possessed by the denser salty water.

All of these observations show that the core is also gaining and losing fluid, but at a much slower rate than the bubble; thus, not only is the bubble fluid slowly entrained but from time to time, the turbulent flow in the bubble tears off a small piece of the core (together with its associated vorticity) and mixes it through the bubble and out into the wake. It is this process which causes the loss of ring impulse. The observations show that, in all cases, the ring remained turbulent during the whole of its motion in our 2 m tank. We suspect that because the Reynolds number of the ring decreases as time progresses (see § 3) the ring could become laminar once some low value of Re has been reached.

Figures 6 and 7 show four alternative ways of looking at these processes; the interested reader is at liberty to choose the one that best suits his tastes. Figure 6(*a*) shows the bubble as a processor of ambient fluid. Ambient fluid enters the interface, mixes with the interior and is rejected to the wake; only a miniscule amount is retained. Figure 6(*b*) shows the average motion of particles as they approach the ring and are either retained or rejected. An alternative view of the entrainment process is shown in figure 7(*b*), where it takes place through a shear layer in much the same way as Maxworthy (1972) proposed for the case of a laminar vortex ring. Finally, figure 7(*a*), as already described, shows the result of propagating a ring through a dyed environment with the resultant mixing and slow penetration of dye into the core.

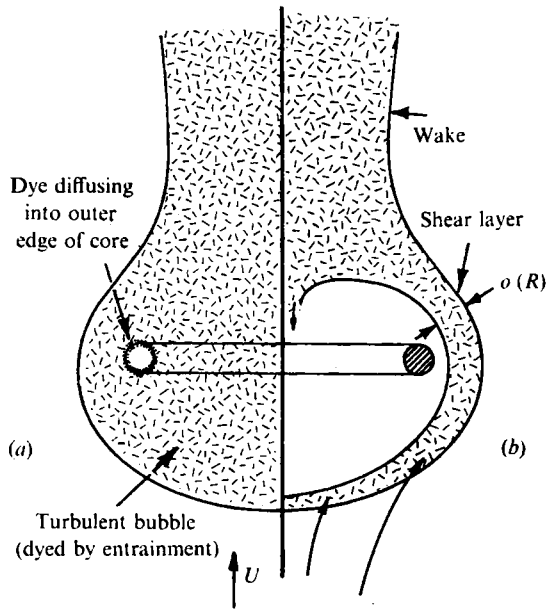

FIGURE 7. (*a*) Showing diagrammatically the process shown photographically in figure 4 (plate 3). Emphasizing the fact that the core remains clear with only a small concentration of dye in its outer surface. (*b*) Showing entrainment taking place through a shear layer with a thickness which is a substantial fraction of the size of the ring.

These observations also make it fairly clear that a straightforward application of vortex-ring dynamics to the disposal of chimney waste (see § 1) cannot be successful. Only if one is able to inject smoke directly into the core itself will the ring transport the pollutant without depositing it into the immediate environment. Experiments on such schemes are at present underway and include the effect of making the density of the core fluid different from that of its surroundings.

3. Vortex-ring model and theory

It has been clear for some time that the information contained in previous measurements was not being interpreted properly. Both the work of Krutsch (1939) and the present author (Maxworthy 1972) had confirmed that the variation of U with x was very close to exponential, or that $U = kt^{-1}$. Such a variation is far enough from that predicted from the assumption of an invariable impulse, i.e. $U = ct^{-\frac{1}{2}}$, that it was clear that some new effect had to be considered.

On the basis of the physical description in the previous section, especially the clear indication of an impulse loss to a wake, we propose the following simple model which includes the effect of this drag force. The turbulent core and its co-travelling bubble are assumed geometrically similar at all times. From an experimental point of view, the most convenient length scale is the distance ($2R$) between the centres of the almost circular core (figures 1 and 6). Therefore, in the theoretical treatment, this quantity will be used as the characteristic dimen-

sion of the ring even though it is smaller than the maximum diameter. It is also convenient to relate the actual geometry of the moving fluid mass to that of a sphere of radius R through some unknown scale factors. As we shall see, this results in a re-definition of the two basic parameters of the problem: an entrainment coefficient α and a drag coefficient C_D''. We assume that the vortex starts at time $t = 0$ with a size $R(0) \equiv R_0$ and an initial velocity $U(0) \equiv U_0$.

Since the flow is turbulent, there is no natural length in the problem except the distance from the origin. This in turn means that the ring must grow linearly with distance. This working hypothesis is shown to agree with our experimental results, and therefore suggests that the turbulent Reynolds number is large enough for viscosity to be unimportant in determining the *gross* properties of the flow. An alternative form of this statement is the so-called entrainment assumption, which linearly relates the rate of growth of bubble volume to its instantaneous surface area and velocity U (cf. Morton, Taylor & Turner 1956):

$$d[\tfrac{4}{3}\pi R^3 k_1]/dt = 4\pi R^3 U \alpha' k_2$$

or

$$dR^3/dt = 3\alpha R^2 U, \tag{1}$$

where $\alpha = \alpha' k_2/k_1$ and k_1 and k_2 are coefficients which relate the actual volume and surface area of the ring to those of an equivalent sphere of radius R. Although this might seem somewhat arbitrary, one can easily show that the same results hold if one considers the volume and surface area of the ring (torus) itself in the calculation.

Similarly, we can write the impulse equation as

$$d[2\pi\rho R^3 U k_3]/dt = -\tfrac{1}{2} C_D'' \rho U^2 \pi R^2 k_4$$

or

$$d[R^3 U]/dt = -\tfrac{1}{4} C_D' U^2 R^2, \tag{2}$$

where $C_D' = C_D'' k_4/k_3$ and k_3 and k_4 are again geometrical coefficients. The right-hand sides of these equations can either be written down by direct analogy with the drag force on a solid body or by calculating the amount of impulse deposited into the wake, cf. Maxworthy (1972).

An immediate result of (1) is, as has already been mentioned,

$$dR/dt = \alpha U,$$

or since

$$U = dx/dt \tag{3}$$

that

$$dR/dx = \alpha. \tag{4}$$

Using (3) in (1) and (2) leads us to

$$dR^3/dx = 3\alpha R^2 \tag{5}$$

and

$$d[R^3 U]/dx = -\tfrac{1}{4} C_D' U R^2. \tag{6}$$

If (6) is expanded and one substitutes from (5) and (4) and integrates from the initial conditions, one gets

$$\int_{U_0}^{U} \frac{dU}{U} = -\int_{R_0}^{R} \left[\frac{C_D'}{4\alpha} + 3\right] \frac{dR}{R}.$$

Integration and simplification gives

$$\overline{U} = \overline{R}^{-\{(C_D'/4\alpha)+3\}}, \tag{7}$$

where $\bar{U} = U/U_0$ and $\bar{R} = R/R_0$. Equations (3) and (4) can be integrated to give

$$\bar{U} = (d\bar{x}/d\bar{t})\,\alpha \tag{8}$$

and

$$\bar{R} = \alpha\bar{x} + 1, \tag{9}$$

where

$$\bar{t} = t/t_c, \quad t_c = R_0/\alpha U_0 \quad \text{and} \quad \bar{x} = x/R_0.$$

We can now combine all of these basic results to get the following set of relationships:

$$\bar{R} = \{[C_D + 4]\,\bar{t} + 1\}^{1/(C_D+4)} = \alpha\bar{x} + 1, \tag{10a,b}$$

$$\bar{U} = \{[C_D + 4]\,\bar{t} + 1\}^{-(C_D+3)/(C_D+4)} = \{\alpha\bar{x} + 1\}^{-(C_D+3)}, \tag{11a,b}$$

where $C_D = C'_D/4\alpha$.

The product $\bar{U}\bar{R}$ is proportional to both the circulation of the ring and its Reynolds number, and is given by

$$\bar{U}\bar{R} = \{[C_D + 4]\,\bar{t} + 1\}^{-(C_D+2)/(C_D+4)} = \{\alpha\bar{x} + 1\}^{-(C_D+2)}.$$

To complete the list of all the useful quantities, we calculate the product $\bar{U}\bar{R}^3$, which is a measure of the impulse remaining in the ring or alternatively the amount lost to the wake (cf. Maxworthy 1972):

$$\bar{U}\bar{R}^3 = \{[C_D + 4]\,\bar{t} + 1\}^{-C_D/(C_D+4)} = \{\alpha\bar{x} + 1\}^{-C_D},$$

which, as we would suspect, becomes constant when $C_D \to 0$.

For long times ($\bar{t} \to \infty$) all of these quantities have power-law asymptotes. When C_D is small, the power law is exceptionally simple:

$$\bar{R} \sim \bar{t}^{\frac{1}{4}}, \quad \bar{U} \sim \bar{t}^{-\frac{1}{4}}, \quad \bar{U}\bar{R} \sim \bar{t}^{-\frac{1}{2}}, \quad \bar{U}\bar{R}^3 \sim \text{constant}.\dagger$$

However, as we have seen and shall see, these are not particularly useful results since the motions of real vortex rings seem to be dominated by the momentum loss effects.

By measuring $\bar{R}$ as a function of $\bar{x}$ we can readily determine α and by measuring $\bar{U}$ as a function $\bar{x}$ we can determine C'_D. Other alternatives would be to measure $\bar{R} = f_1(\bar{t})$ or $\bar{U} = f_2(\bar{t})$ or make use of the relationship between $\bar{t}$ and $\bar{x}$, namely

$$[C_D + 4]\,\bar{t} + 1 = [\alpha\bar{x} + 1]^{C_D+4}.$$

These latter depend on C_D in a more complicated way and are not so convenient to use except as checks on the consistency of the measurements.

From our previous comments, it is clear that both α and C'_D depend on the turbulent processes occurring in the core. One would hope that the latter are independent of the Reynolds number of the ring and that α and C'_D are universal constants for all well-formed rings.

4. Experimental results and comparison with theory

In order to test the model proposed in the previous section, we performed a series of tests in which R and U were measured as functions of x and t. Data were recorded photographically by a camera that was traversed downwards at the

† The fact that the circulation decreases while the impulse does not is, of course, attributable to the fact that vorticity is still being cancelled at the centre-line of the ring even though none is deposited into a wake.

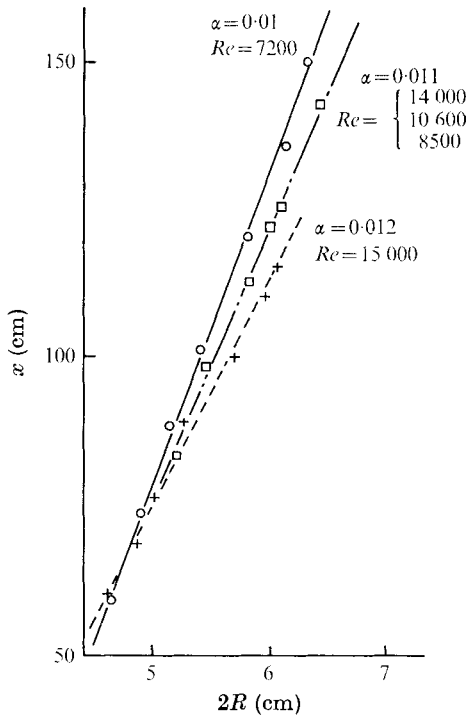

FIGURE 9. Ring diameter $2R$ as a function of distance traversed x, for various Reynolds numbers.

same speed as the ring, thus reducing parallax effects and giving a large image of the ring. Figure 8 (plate 4) shows examples of such experiments. Initial Reynolds numbers Re_1† varied between 14000 and 30000.

From the measurements of R *vs.* x (figure 9), the value of α could immediately be found. Values varied between the extreme values, 0·01 and 0·012, shown. A large amount of data clustered around $\alpha = 0{\cdot}011$ but most of this has been suppressed for the sake of clarity. We believe that there was no strong trend with Reynolds number, for despite the small absolute increase in the size of the bubble and the suspicion that this means that the flow could still be dependent on initial conditions, the bubble has actually processed an enormous quantity of fluid; in fact, practically all it has encountered during its motion.

The velocity data were then reduced according to the prescription indicated in (11*b*), i.e.,

$$\overline{U} = [\alpha\bar{x} + 1]^{-(C_D+3)}.$$

From the slope of these curves (figure 10) values of C_D between 1·8 and 2·7 were found; these reduced to values of C'_D between 0·084 and 0·108 for the drag coefficient of the equivalent sphere. The drag coefficient based on the diameter

† Two Reynolds numbers can be conveniently defined. The first, $Re_1 = U_e D_e/\nu$, was that calculated using the vortex velocity and diameter as it left the exit hole. The second, $Re_2 = U_0 D_0/\nu$, was based on values measured at the beginning of the final turbulent ring phase and varied between 14400 and 6500.

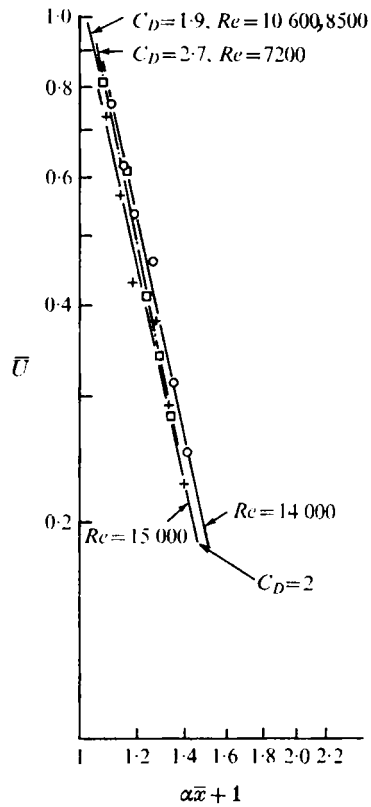

FIGURE 10. Ring velocity $\bar{U}$ as a function of the distance $\alpha\bar{x}+1$.

of the actual moving fluid mass will obviously be much smaller than this, since, like a Hill's spherical vortex, the ratio of total diameter to diameter between centres of rotation is approximately $\frac{2}{3}$ in our case. The drag coefficient based on the frontal area of the moving bubble is thus estimated to be $0{\cdot}04 \pm 0{\cdot}005$. This is to be compared with the value of 0·23 for a solid sphere when the boundary layer is turbulent before separation, i.e. in the transcritical regime (Maxworthy 1969). Again, there was no discernable trend with Reynolds number. However, it is clear from the error estimates that the accuracy of the experiments was not very high and that a Reynolds number trend could be hidden therein. It is, however, significant that the Reynolds number was decreasing throughout the course of any one experiment and yet there was no departure from a linear dependence of size on distance. At some later stage, the ring probably becomes laminar when its Re falls below some maximum critical value. (The value of 600 found in Maxworthy (1972) is one possible candidate for this value.) The present experiments did not continue long enough for this stage to be reached.

5. Conclusions and discussion

We thus conclude that the motions of real vortex rings depend critically on two fundamental concepts. The first, that of entrainment, is already quite familiar, although in this case accepted concepts must be modified to account for the strong constraints placed upon the turbulence by rotation. Thus, the controlling entrainment rate within the core is only slightly larger than that due to molecular diffusion alone. As we have shown, the entrainment rate for the whole bubble is much larger than this, with the result that most of the entrained fluid is rejected to a wake. This second concept of rejection or detrainment is probably only of consequence in some classes of unsteady flow in which there is a turbulent interface to the rear of a large turbulent fluid mass. In the present case, the vorticity contained within the ring is slowly deposited into the wake along with the detrained fluid. This also means that the ring impulse must decrease to appear as a momentum defect in the wake. We have found that the drag force on the body that this represents is equivalent to assigning a drag coefficient of $0{\cdot}04 \pm 0{\cdot}005$ to the motion, where this drag coefficient is obtained by normalizing the drag force with the dynamic pressure of the approaching stream multiplied by the frontal area of the moving fluid mass.

As previously mentioned, our results appear to disagree with those of Johnson (1970, 1971) for ranges of parameters (i.e. Reynolds numbers and distance) that do not seem to be greatly different. Two points stand out: one is his relationship $2R/D = K_1[(x-x_v)/D]^{\frac{1}{3}}$, where D is the orifice diameter. However, it appears that some of his data were taken before the initial instability phase was over (i.e. before $x/D \approx 15$) and therefore before the final similarity phase had been reached. These points tend to weight his data away from agreement with ours. We have attempted to plot his data, in the similarity range, as accurately as possible, and it seems that they basically agree with ours. The other difficulty concerns his statement that momentum (presumably impulse) is conserved. With a wake present, this is clearly impossible although the accuracy of his data reduction scheme might have to be very high for the difference to be clearly revealed. One should also observe that it is not possible to use his method to make predictions of ring motion because none of the additive constants he derives can be logically related to some basic characteristic of the ring (e.g. its Reynolds number). Our scheme on the other hand can be used predictively once a set of initial conditions has been specified somewhere in the similarity region of motion.

We gratefully acknowledge the National Science Foundation for its support of this work under Grant GK-19107 to the University of Southern California.

Appendix. An extended theory of laminar vortex rings

We extend the analysis previously presented in Maxworthy (1972) to take account explicitly of the momentum loss to a wake, i.e. an equivalent drag force on the laminar vortex ring.

The equations to be solved are a mass entrainment equation and a momentum

equation that equates the rate of change of the impulse of the vortex ring to the impulse loss it experiences. If R and U are measures of the size of the ring and its velocity, then these equations are

$$dR^3/dt = \gamma\nu^{\frac{1}{2}}R^{\frac{3}{2}}U^{\frac{1}{2}}, \tag{A 1}$$

$$d(UR^3)/dt = -\beta\nu^{\frac{1}{2}}R^{\frac{1}{2}}U^{\frac{3}{2}}, \tag{A 2}$$

where γ and β are constants with values of order unity.

Let

$$R = c_1 t^m, \quad U = c_2 t^n. \tag{A 3}$$

By substituting (A 3) in (A 1) and (A 2) and equating exponents of t, we find that $m = \frac{1}{3}n + \frac{2}{3}$.

By equating the coefficients of t in (A 2), for example, we eventually find an expression for n which includes the viscous effects we wish to observe and shows explicitly how the Reynolds number of the flow enters our original calculation (Maxworthy 1972, p. 27). Thus

$$U = c_1 t^{-\frac{1}{2}\beta Re_0^{-\frac{1}{2}}\tau_0 - 1},$$

where $Re_0 = U_0R_0/\nu$ (with U_0 and R_0 the initial velocity and size of the vortex ring) and $\tau_0 = t_0U_0/R_0$ (t_0 is the time that has elapsed from the formation of the ring at a virtual origin to the time at which it is observed in the experiment, i.e., formed with a finite size at the orifice (Maxworthy 1972, p. 28)). In the experiments reported previously t_0 had a value of, typically, 10 s while U_0 and R_0 were in the ranges 2–10 cm/s and 2–3 cm, respectively. Thus, the quantity $\epsilon = -\frac{1}{2}\beta Re_0^{-\frac{1}{2}}\tau_0$ has a range of values from about 0·1 at high values of Re_0 to about 0·5 at low values. The variation in velocity of the ring will then start out close to the relationship $U \sim t^{-1}$, as in Maxworthy (1972), but deviate more and more from this law as time progresses, as was found experimentally. Perhaps this result can be most readily seen by considering the variation of distance x travelled with t. We find for small values of ϵ that

$$x \sim \log t - \tfrac{1}{2}\epsilon(\log t)^2 + \ldots.$$

This first term again represents the experimental variation found previously while the correction term shows the effect of impulse loss to the wake as we have already crudely estimated.

REFERENCES

JOHNSON, G. M. 1970 Researches on the propagation and decay of vortex rings. *Aero. Res. Lab., Wright-Patterson A.F.B., Rep.* ARL 70-0093.

JOHNSON, G. M. 1971 An empirical model of the motion of turbulent vortex rings. *A.I.A.A. J.* **9**, 763.

KRUTSCH, C.-H. 1939 Über eine experimentelle beobachtete Erscheinung an Wirbelringen bei ihrer translatorischen Bewegung in wirklichen Flüssigkeiten. *Ann. Phys.* **35**, 497.

MAXWORTHY, T. 1969 Experiments on the flow around a sphere at high Reynolds numbers. *J. Appl. Mech.* E **36**, 598.

MAXWORTHY, T. 1972 The structure and stability of vortex rings. *J. Fluid Mech.* **51**, 15.

MORTON, B. R., TAYLOR, G. I. & TURNER, J. S. 1956 Turbulent gravitational convection from maintained and instantaneous sources. *Proc. Roy. Soc.* A **234**, 1.

SULLIVAN, J. P., WIDNALL, S. E. & EZEKIEL, S. 1973 A study of vortex rings using a laser doppler velocimeter. *A.I.A.A. J.* **11**, 1384.

TURNER, J. S. 1960 On the intermittent release of smoke from chimneys. *Mech. Engng Sci.* **2**, 356.

WIDNALL, S. E. & SULLIVAN, J. P. 1973 On the stability of vortex rings. *Proc. Roy. Soc.* A **332**, 335.

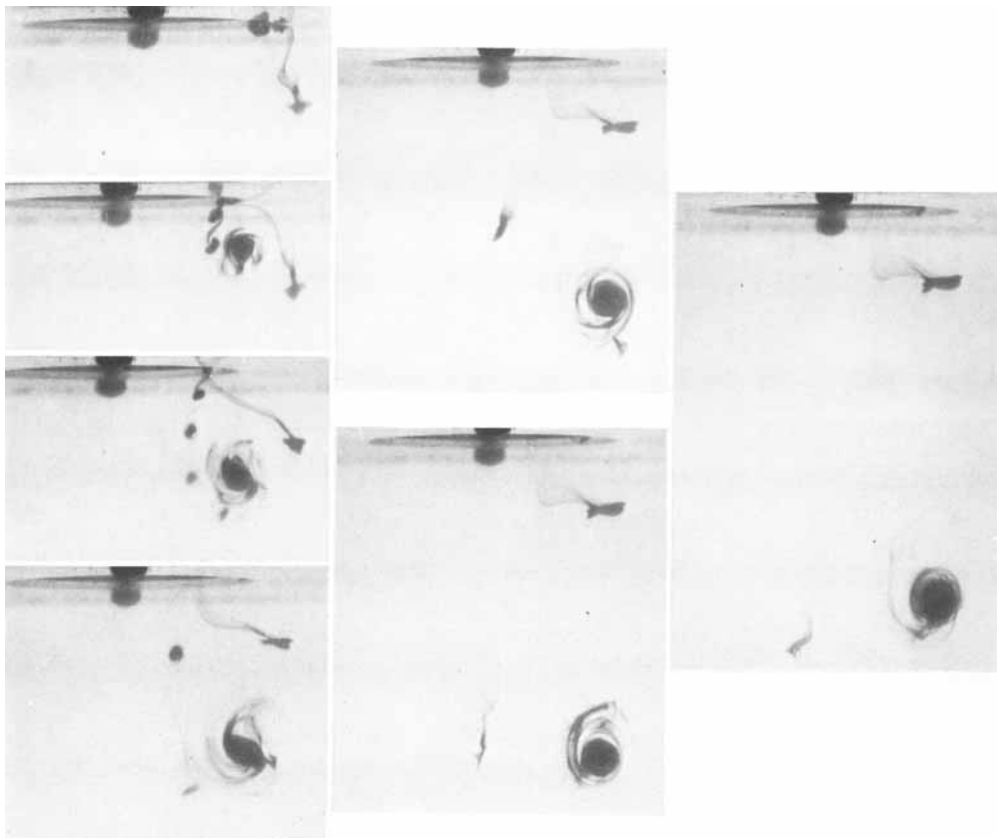

FIGURE 2. Vortex ring being formed at a sharp edge. Dye was introduced into just a small portion of the whole circumference of the ring. Formation and coalescence of small vortices is clearly shown. At the later turbulent phase, this small amount of dye was diffused through the whole length of the vortex core.

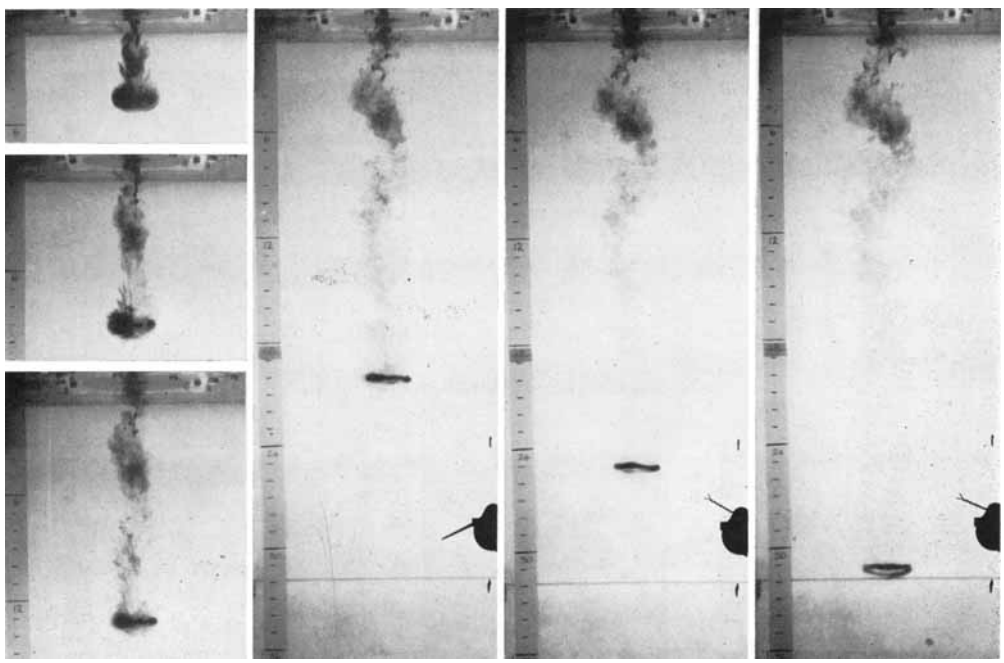

FIGURE 3. A large blob of dye was introduced by the piston motion. Most of the dye was left behind in a wake with only a small amount trapped in the turbulent core; because more dye was introduced to the left side of the ring initially, it retained dye for a larger distance than the right side.

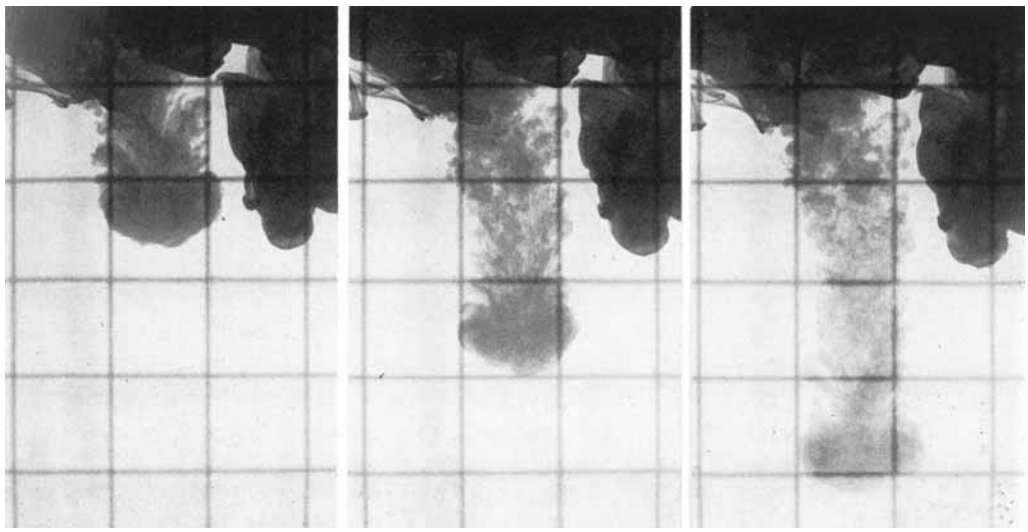

FIGURE 4. Entrainment by a turbulent ring. An undyed ring was pulsed through a region of dye. It entrained some and then left it behind in a wake.

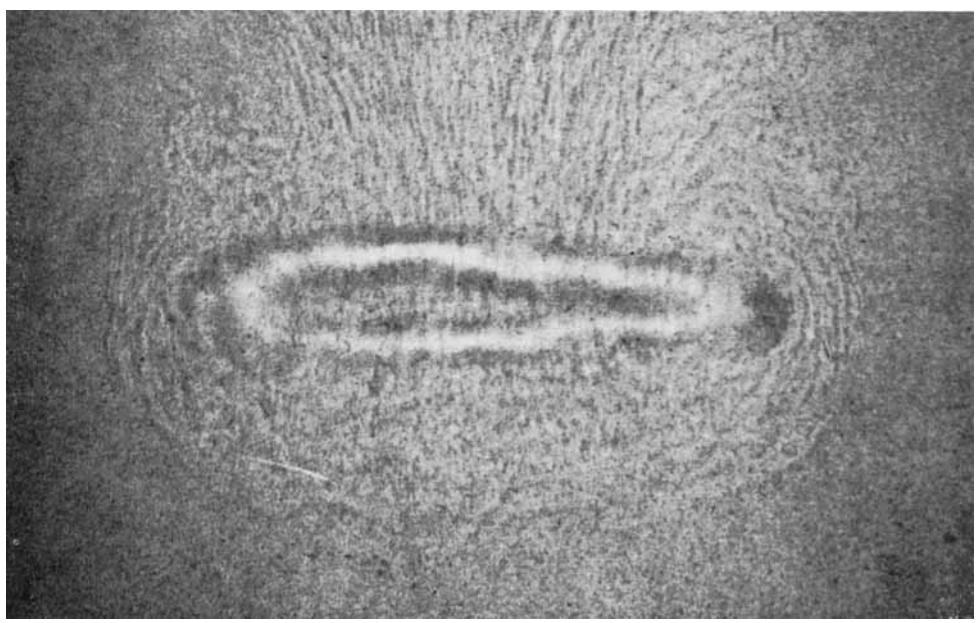

FIGURE 5. A 'shadowgraph' photograph of a vortex bubble. The flow has been made visible by lightly seeding the flow with a dilute salt solution. Although the difference in turbulence scales cannot be seen very clearly in this photograph, visual observations show them very clearly. However, the outer limits of the bubble and wake can be seen as can the interface between the ring and bubble.

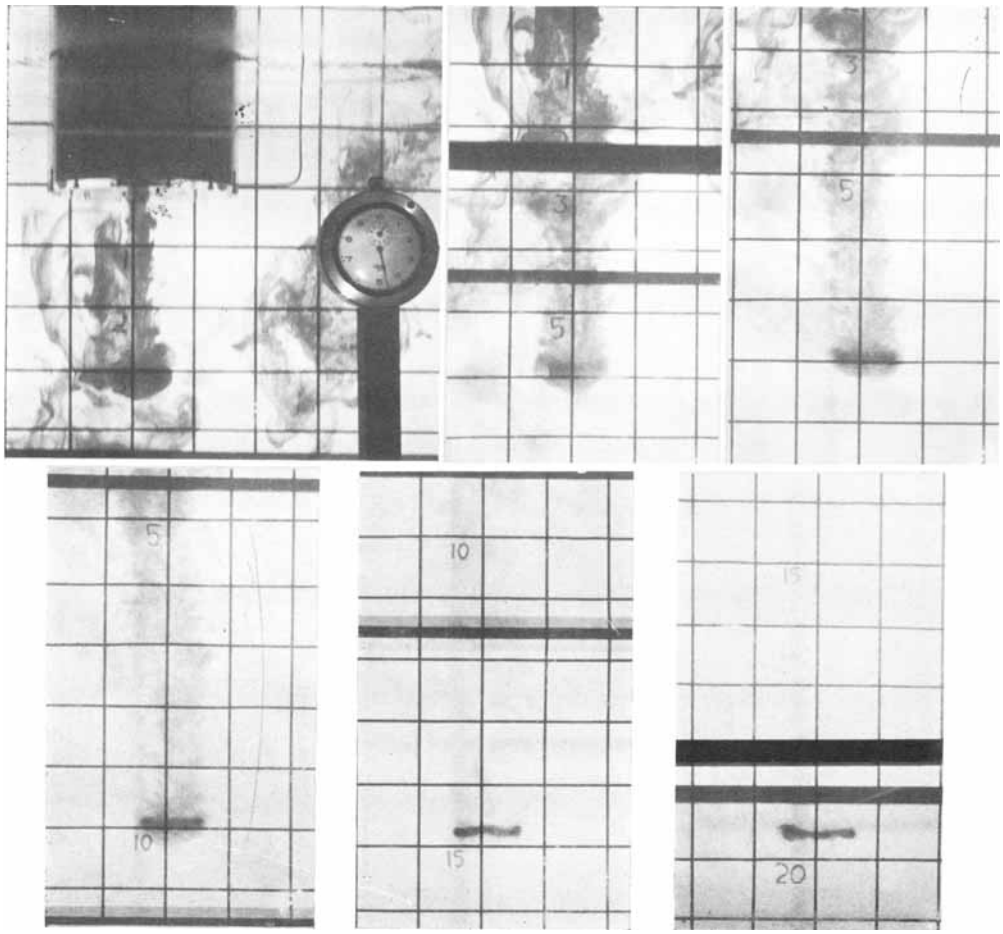

FIGURE 8. A series of photographs taken by a camera being traversed at the same speed as the ring.